LINC01605 knockdown induces apoptosis in human Tenon's capsule fibroblasts by inhibiting autophagy

QIFEI SHANG, YANHUA YANG and HANGZHU LI

Department of Ophthalmology, Fuyang People's Hospital, Hangzhou, Zhejiang 311400, P.R. China

Received July 5, 2021; Accepted January 25, 2022

DOI: 10.3892/etm.2022.11273

Abstract. Glaucoma is an irreversible disease that causes blindness. Formation of a hypertrophic scar (HS) is the main cause of failure of glaucoma surgery. The long non-coding RNA LINC01605 is closely associated with the formation of HS; however, the function of LINC01605 in the formation and development of HS remains unclear. For this study, firstly, human Tenon's capsule fibroblasts (HTFs) and corneal epithelial cells (control cells) were collected from patients (n=5) with POAG who underwent glaucoma filtration surgery at Fuyang People's Hospital. Immunofluorescence analysis was performed to detect the expression levels of vimentin (one of the main components of medium fiber and plays an important role in the cytoskeleton and motility), keratin (the main component of cytoskeletal proteins) and LC3 (an autophagy marker). In addition, reverse transcription-quantitative PCR analysis was performed to detect LINC01605 expression. Besides, the Cell Counting Kit-8 assay was performed to assess the viability of human Tenon's capsule fibroblasts (HTFs). Next, flow cytometry was performed to detect HTF apoptosis. Furthermore, western blot analysis was performed for Bax, Bcl-2, Pro-caspase-3, cleaved caspase-3, phosphorylated (p-)Smad2, Smad2, α-SMA, MMP9, ATG7, p62, beclin 1, p-AMPK and AMPK in HTFs to determine the mechanism by which LINC01605 regulates the formation and development of HS. Moreover, a Transwell assay was performed to detect the migratory ability of HTFs. The results demonstrated that LINC01605 was significantly upregulated in HS tissues compared with that in normal (control/healthy) tissues. In addition, vimentin was highly expressed in HTFs, whereas keratin was expressed at a low level. Also, in HTFs, LINC01605 knockdown inhibited cell viability by inducing apoptosis, decreasing Smad2 activation and inhibiting autophagy. Furthermore, LINC01605 knockdown significantly inhibited the migratory ability of HTFs. Transfection with LINC01605 small interference RNAs significantly downregulated the expression levels of p-Smad2, α-SMA and MMP9 in HTFs. Furthermore, LINC01605 knockdown notably inhibited the viability and migration, and induced the apoptosis of HTFs, the effects of which were reversed following treatment with TGF-β. Taken together, the results of the present study suggested that LINC01605 knockdown may inhibit the viability of HTFs by inducing the apoptotic pathway. These findings may provide novel directions for the treatment of HS.

Correspondence to: Dr Qifei Shang, Department of Ophthalmology, Fuyang People's Hospital, 429 Beihuan Road, Fuchun Street, Fuyang, Hangzhou, Zhejiang 311400, P.R. China
E-mail: jayffi@163.com

Key words: hypertrophic scar, LINC01605, apoptosis, Smad2, autophagy

Introduction

Glaucoma is a common eye disease caused by optic nerve atrophy and visual field defect (1). Primary glaucoma comprises angle-closure glaucoma and open-angle glaucoma (2); the most common type of glaucoma is primary open-angle glaucoma (POAG) (3). Glaucoma is the leading cause of irreversible vision loss and blindness (2). The condition affects >2 million individuals annually in the United States (4). According to the World Health Organization, the number of glaucoma patients worldwide was predicted to reach 79.6 million by 2020, of which 11.2 million may eventually develop blindness in both eyes (4,5). As of 2011, 2.7 million patients in the United States suffered from POAG alone, and the number of patients with POAG is projected to increase to >7 million by the year 2050 (5). The formation of a hypertrophic scar (HS), which is characterized by excessive proliferation of fibroblasts, can lead to the failure of glaucoma filtration surgery (6,7). Currently, the major treatments for HS include medication, surgery and physical therapy (8); however, the outcomes are not yet satisfactory. Thus, further studies are required to identify effective treatment strategies for HS.

Long non-coding RNAs (lncRNAs) are a class of non-coding RNA molecules of >200 nucleotides in length that are located in the nucleus or in the cytoplasm and have no or little protein coding function (9). lncRNAs are extensively involved in various signaling pathways that influence epigenetics, cell cycle, proliferation (10). In addition, abnormal lncRNA expression or function is closely associated with the occurrence of human diseases, including glaucoma (11,12). For example, Nong *et al* (13) reported that lncRNA COL1A2-AS1 was highly expressed in HS and fibroblasts, and that it inhibited the proliferation of fibroblasts by promoting Smad7 expression. In addition, Li *et al* (14) demonstrated that lncRNA8975-1 was

highly expressed in HS tissues and could inhibit fibroblast proliferation and α-smooth muscle actin (α-SMA) expression. Zhu *et al* (15) reported that the lncRNA LINC01605 is closely associated with the formation of HS and is expressed at abnormally high levels in human dermal fibroblasts. However, the molecular mechanism by which LINC01605 may regulate the development of HS remains unclear.

Therefore, present study aimed to investigate the role of LINC01605 in HS to identify novel potential treatment strategies. To explore the effects of LINC01605 on the formation of HS, human Tenon's capsule fibroblasts (HTFs) and corneal epithelial cells (control cells) were collected and cultured *in vitro*. For this study, CCK-8, flow cytometry and Transwell assays were conducted to detect the viability, apoptosis and migratory of HTFs, respectively.

Materials and methods

Specimen collection, isolation of HTFs and cell culture. The inclusion criteria for the patients with glaucoma included in the present study were as follows: i) Patients diagnosed with glaucoma according to the latest diagnostic criteria for glaucoma developed by the Cooperative Group on Fundus Diseases of the People's Republic of China (6); and ii) patients who have undergone glaucoma surgery. Patients were excluded based on the following criteria: i) Patients with other diseases and currently receiving treatment; ii) pregnant or breast-feeding women; iii) patients who are allergic to probiotics or who have recently used/are using antibiotics; iv) patients with alcoholism (individuals who drink ≥5 bottles of beer at a time or have a blood alcohol level of ≥0.08 g/100 ml); and v) smokers, according to a previous reference (6).

Matched HS and normal (control/healthy) tissues were collected from patients (n=5) with POAG who underwent glaucoma filtration surgery at Fuyang People's Hospital (Hangzhou, China) between November 2019 and May 2020 according to previous reports (16,17). It has been reported that HS tissue has more melanocytes, and that there are fewer melanocytes in normal tissue (18). The basic clinicopathological characteristics of the patients are listed in Table I. Subsequently, to isolate HTFs from HS tissues and corneal epithelial cells (control cells) from healthy tissues. Briefly, 5x5-mm sections of Tenon's capsule were collected, minced and placed in a 35-mm culture dish containing Dulbecco's modified Eagle's medium (DMEM; Invitrogen; Thermo Fisher Scientific, Inc.) supplemented with 10% fetal calf serum (Invitrogen; Thermo Fisher Scientific, Inc.), 50 U/ml penicillin and 50 μg/ml streptomycin (Invitrogen; Thermo Fisher Scientific, Inc.). Cells were allowed to migrate from the explanted tissue and were then incubated at 37˚C in 5% CO_2. Cells between the third and fifth passages were used according to a previous study (19). Next, HTFs were maintained in DMEM supplemented with 10% FBS, 1% penicillin and 1% streptomycin (all from Thermo Fisher Scientific, Inc.) at 37˚C with 5% CO_2, as previously described (20,21). The isolated cells were observed using fluorescent staining under a fluorescence microscope (Olympus Corporation). The present study was approved by the Ethics Committee of Fuyang People's Hospital (Hangzhou, China; approval no. FPH20191011), and written informed consent was provided by all patients prior to the study onset.

Reagents. 3-Methyladenine (3-MA) was obtained from MedChemExpress (cat. no. HY-19312). Cells were treated with 1 mmol/l 3-MA for 24 h according to a previous study (22). In addition, TGF-β was provided by Millipore Sigma (cat. no. SAB4502954). Cells were treated with 10 ng/ml TGF-β for 24 h according to a previous study (23).

Reverse transcription-quantitative PCR (RT-qPCR). Total RNA was extracted from HS tissues, healthy tissues and HTFs ($5x10^4$/ml) using TRIzol® reagent (Invitrogen; Thermo Fisher Scientific, Inc.). Total RNA was reverse transcribed into cDNA using the EntiLink™ 1st Strand cDNA Synthesis kit [ELK (Wuhan) Biotechnology Co., Ltd.] according to the manufacturer's instructions. qPCR was subsequently performed using the StepOne™ Real-Time PCR System (Thermo Fisher Scientific, Inc.). EnTurbo™ SYBR Green PCR SuperMix kit (ELK Biotechnology Co., Ltd.) was used for qPCR. The thermocycling conditions were used as follows: 3 min at 95˚C, followed by 40 cycles of 10 sec at 95˚C, 30 sec at 58˚C and 30 sec at 72˚C. mRNA expression levels were normalized to β-actin levels. Relative expression levels were calculated using the $2^{-\Delta\Delta Cq}$ method (24). The following primer sequences were used for qPCR: β-actin forward, 5'-GTCCACCGCAAATGCTTCTA-3' and reverse, 5'-TGCTGTCACCTTCACCGTTC-3'; and LINC01605 forward, 5'-CAACTCATTCCCGTTACAAACA-3' and reverse, 5'-CATCTCAACTGCCTCTGTCTCC-3'.

Immunofluorescence analysis. Droplets of suspended corneal epithelial cells and HTFs ($3x10^5$ cells/well) were cultured in a 24-well plate at 37˚C with 5% CO_2 and subsequently fixed with 4% paraformaldehyde for 30 min at room temperature. The following primary antibodies were diluted with 5% BSA (Beyotime Biotechnology): Anti-vimentin (1:1,000; Abcam; cat. no. ab92547), anti-keratin (1:1,000; Abcam; cat. no. ab8068) and anti-LC3 (1:1,000; Abcam; cat. no. ab192890) at 4˚C. Following primary antibody incubation overnight at 4˚C, cells were incubated with horseradish peroxidase IgG secondary antibody (1:5,000; Abcam; cat. no. ab6728) for 1 h at room temperature. Cells were washed three times with PBS. Cell nuclei were stained with 50-100 μl DAPI at room temperature for 5 min. Finally, cells were observed under a fluorescence microscope (Olympus Corporation).

Small interference (si)RNA transfection. Three siRNAs against LINC01605 and an siRNA-negative control (NC) were synthesized by Guangzhou RiboBio Co., Ltd. The following sequences were used: LINC01605 siRNA1, 5'-TCTTGAAGAATAAGAAGCCACAGCT-3'; LINC01605 siRNA2, 5'-GAGTCTTGAAGAATAAGAAGCCACA-3'; LINC01605 siRNA3, 5'-TAAGAAGCCACAGCTTGTCAGGGAA-3'; and siRNA-NC, 5'-GAGGTTGAATAAGAAGAACCTCACA-3'. The siRNAs (10 nM) were transfected into HTFs ($3x10^5$ cells/well) using Lipofectamine® 2000 reagent (Thermo Fisher Scientific, Inc.) for 48 h at 37˚C. After 48 h of incubation, cells were used for subsequent experimentation. The blank group was comprised of non-transfected cells.

Cell viability assay. The Cell Counting Kit-8 (CCK-8) assay (Beyotime Institute of Biotechnology) was performed to

Table I. Basic clinicopathological characteristics of the patients.

Patient	Age, years	Sex	Date of hospital admission, month/year
1	67	Female	11/2019
2	72	Male	11/2019
3	54	Female	03/2020
4	62	Female	04/2020
5	71	Male	05/2020

assess cell viability. HTFs were seeded into 96-well plates at a density of $5x10^3$ cells/well. Next, siRNA-NC, LINC01605 siRNA1 and LINC01605 siRNA2 were transfected into HTFs using Lipofectamine® 2000 reagent for 6 h at 37˚C. The culture medium was then changed and HTFs continued to be cultured in DMEM for 0, 24, 48 and 72 h. Next, 10 μl CCK-8 reagent was added into each well and cells were incubated for 2 h at 37˚C. Absorbance was measured at a wavelength of 450 nm using a microplate reader (Varioskan™ LUX; Thermo Fisher Scientific, Inc.).

Apoptosis analysis. Apoptosis was analyzed by flow cytometry. HTFs were seeded into six-well plates at a density of $5x10^4$ cells/ml. Following transfection with siRNAs, cells were stained with Annexin V-FITC and PI (Tianjin Sungene Biotech, Co., Ltd.) for 15 min in the dark at room temperature. Subsequently, the apoptotic rate (the sum of early and late apoptosis) was analyzed using a FACSCanto II flow cytometer (BD Biosciences). The data was analyzed using FlowJo software (version 10.6.2; FlowJo LLC).

Western blotting. Protein was extracted from HTFs using RIPA buffer (Aspen Biotechnology) and concentration was determined using a BCA kit (Aspen Biotechnology, Co., Ltd.). Proteins (30 μg/lane) were separated by 10% SDS-PAGE, transferred onto PVDF membranes and blocked with 5% non-fat milk diluted in TBS with 0.1% Tween-20 for 1 h at room temperature. The membranes were incubated overnight at 4˚C with primary antibodies against Bax (1:1,000; Abcam; cat. no. ab32503), Bcl-2 (1:1,000; Abcam; cat. no. ab32124), Pro-caspase-3 (1:1,000; Abcam; cat. no. ab32150), cleaved caspase-3 (1:1,000; Abcam; cat. no. ab2302), phosphorylated (p)-Smad2 (1:1,000; Abcam; cat. no. ab280888), Smad2 (1:1,000; Abcam; cat. no. ab40855), α-SMA (1:1,000; Abcam; cat. no. ab5694), MMP9 (1:1,000; Abcam; cat. no. ab76003), autophagy-related (ATG)7 (1:1,000; Abcam; cat. no. ab52472), p62 (1:1,000; Abcam; cat. no. ab109012), beclin 1 (1:1,000; Abcam; cat. no. ab207612), p-AMP-activated protein kinase (AMPK) (1:1,000; Abcam; cat. no. ab133448), AMPK (1:1,000; Abcam; cat. no. ab32047) and β-actin (1:1,000; Abcam; cat. no. ab8227). Subsequently, the membranes were incubated with horseradish peroxidase (HRP)-labeled goat anti-rabbit secondary antibody (1:5,000; cat. no. ab7090; Abcam) at room temperature for 1 h. Protein bands were visualized using the Enhanced Chemiluminescence Reagent (Thermo Fisher Scientific, Inc.). β-actin was used as a loading control. Finally, the density of the blots was analyzed using AlphaEaseFC software (version 4.0; Alpha Innotech Corporation).

Transwell migration assay. The Transwell migration assay was performed using 24-well Transwell chambers (Corning, Inc.). Firstly, HTFs during the logarithmic growth phase were incubated overnight at 37˚C. Next, HTFs were transfected with siRNA-NC, LINC01605 siRNA1 and LINC01605 siRNA2 using Lipofectamine 2000 reagent for 24 h at 37˚C. After that, HTFs (200 μl) were plated on the upper chamber suspended with 100 μl serum-free DMEM at 37˚C, and 600 μl complete DMEM supplemented with 10% FBS was added to the lower chamber; cells were incubated for 24 h at 37˚C. Following incubation, the migrated cells on the lower chamber were stained with 0.2% crystal violet at room temperature for 30 min and observed under a light microscope (Leica Microsystems Ltd.; cat. no. DMLB2).

Statistical analysis. Statistical analysis was performed using GraphPad Prism software (v7.0; GraphPad Software, Inc.). All experiments were performed in triplicate. The comparison between two matched samples was analyzed with paired Student's t-test. One-way ANOVA followed by Tukey's post hoc test was used to compare differences between multiple groups. All experimental data are presented as the mean ± SD. $P<0.05$ was considered to indicate a statistically significant difference.

Results

HTFs are successfully isolated and LINC01605 knockdown decreases the viability of HTFs successfully isolated from patients with POAG. Matching HS and healthy tissues were collected from patients with POAG who underwent glaucoma filtration surgery at Fuyang People's Hospital, and RT-qPCR analysis was performed to detect LINC01605 expression levels. The results demonstrated that LINC01605 expression was higher in HS tissues compared with that in normal (control/healthy) tissues (Fig. 1A). Subsequently, HTFs and corneal epithelial cells were isolated from the aforementioned tissues. In addition, it has been reported that vimentin is a fibrocyte marker (25). Vimentin is one of the main components of medium fiber and plays an important role in cytoskeleton and motility (26,27). Furthermore, keratin is the main component of cytoskeletal proteins (28). Immunofluorescence assays indicated that vimentin was highly expressed in HTFs and in corneal epithelial cells, whereas keratin was expressed at a low level in HTFs (Fig. 1B).

LINC01605 expression significantly decreased in HTFs following transfection with LINC01605 siRNAs (Fig. 1C). The results indicated that LINC01605 siRNA1 and LINC01605 siRNA2 had a stronger knockdown effect compared with LINC0165 siRNA3, thus these two siRNAs were selected for subsequent experiments (Fig. 1C). LINC01605 siRNA1 and LINC01605 siRNA2 significantly inhibited the viability of HTFs compared with siRNA-NC (Fig. 1D). These results suggested that HTFs were successfully isolated and LINC01605 siRNA significantly inhibited the viability of HTFs.

LINC01605 knockdown induces apoptosis in HTFs. To investigate the function of LINC01605 in HTFs, flow cytometry

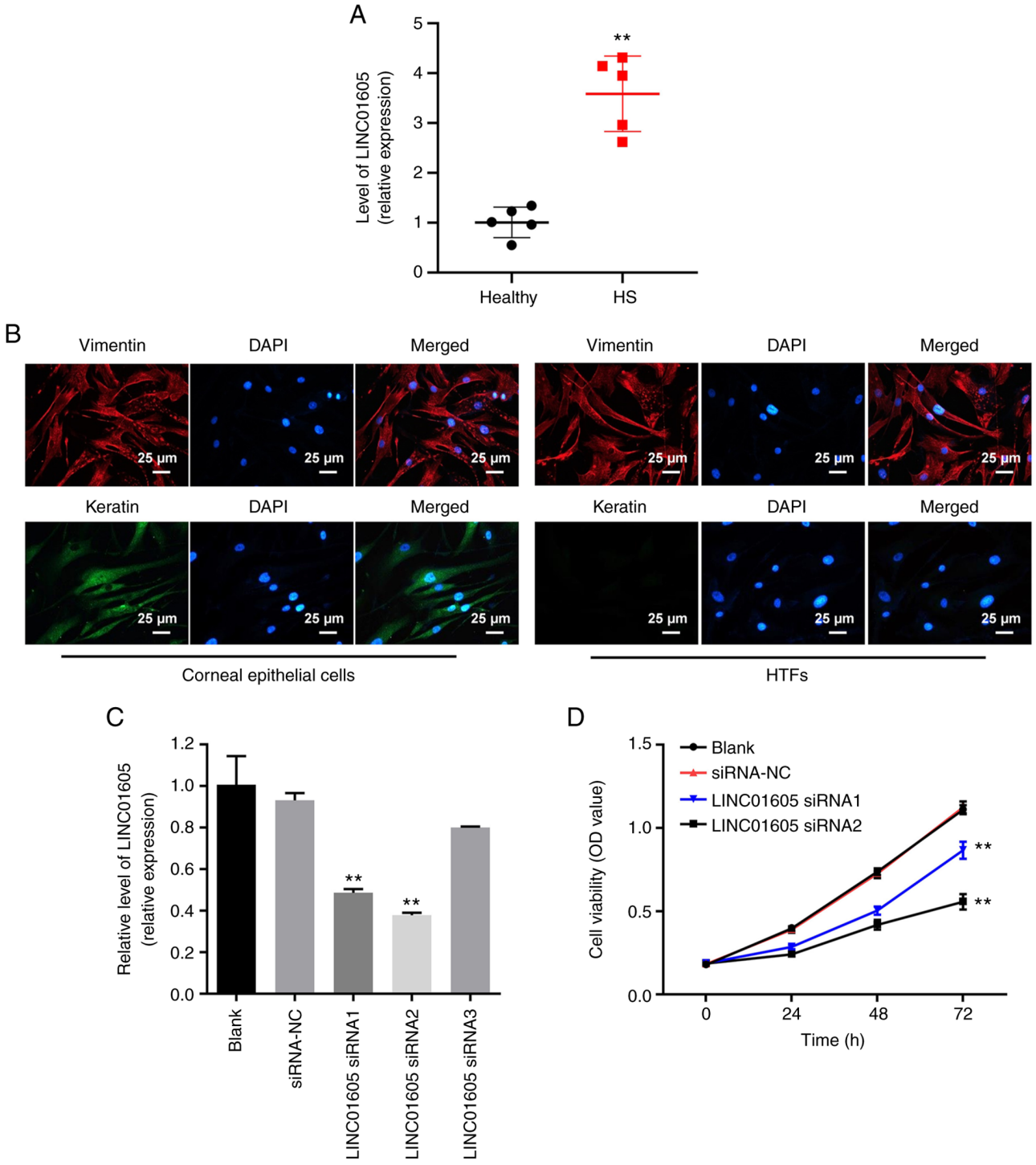

Figure 1. Successful isolation of HTFs and LINC01605 knockdown significantly inhibits the viability of HTFs from patients with POAG. (A) RT-qPCR was performed to detect the expression of LINC01605 in HS or normal (control/healthy) corneal tissues. (B) Immunofluorescence staining was performed to detect the expression of vimentin and keratin in corneal epithelial cells and HTF. Scale bar, 25 μm. (C) HTFs were transfected with siRNA-NC, LINC01605 siRNA1, LINC01605 siRNA2 or LINC01605 siRNA3, and RT-qPCR was performed to detect the expression levels of LINC01605. (D) Cell Counting Kit-8 assay was used to detect the viability of HTFs. n=3; **P<0.01 vs. siRNA-NC or healthy/blank group. HS, hypertrophic scar; HTFs, human Tenon's capsule fibroblasts; NC, negative control; OD, optical density; POAG, primary open-angle glaucoma; RT-qPCR, reverse transcription-quantitative PCR; siRNA, small interfering RNA.

was performed. As presented in Fig. 2A, LINC01605 knockdown significantly induced apoptosis in HTFs compared with the siRNA-NC or blank group. In addition, transfection with LINC01605 siRNAs notably increased the expression levels of apoptosis-related proteins Bax and cleaved caspase-3, and decreased Bcl-2 expression in HTFs, compared with the siRNA-NC or blank group (Fig. 2B). Collectively, these results suggested that LINC01605 knockdown significantly induced apoptosis in HTFs.

LINC01605 knockdown inhibits the migration of HTFs. Transwell assays were performed to investigate the effect of LINC01605 on the migratory ability of HTFs. The results demonstrated that LINC01605 knockdown significantly

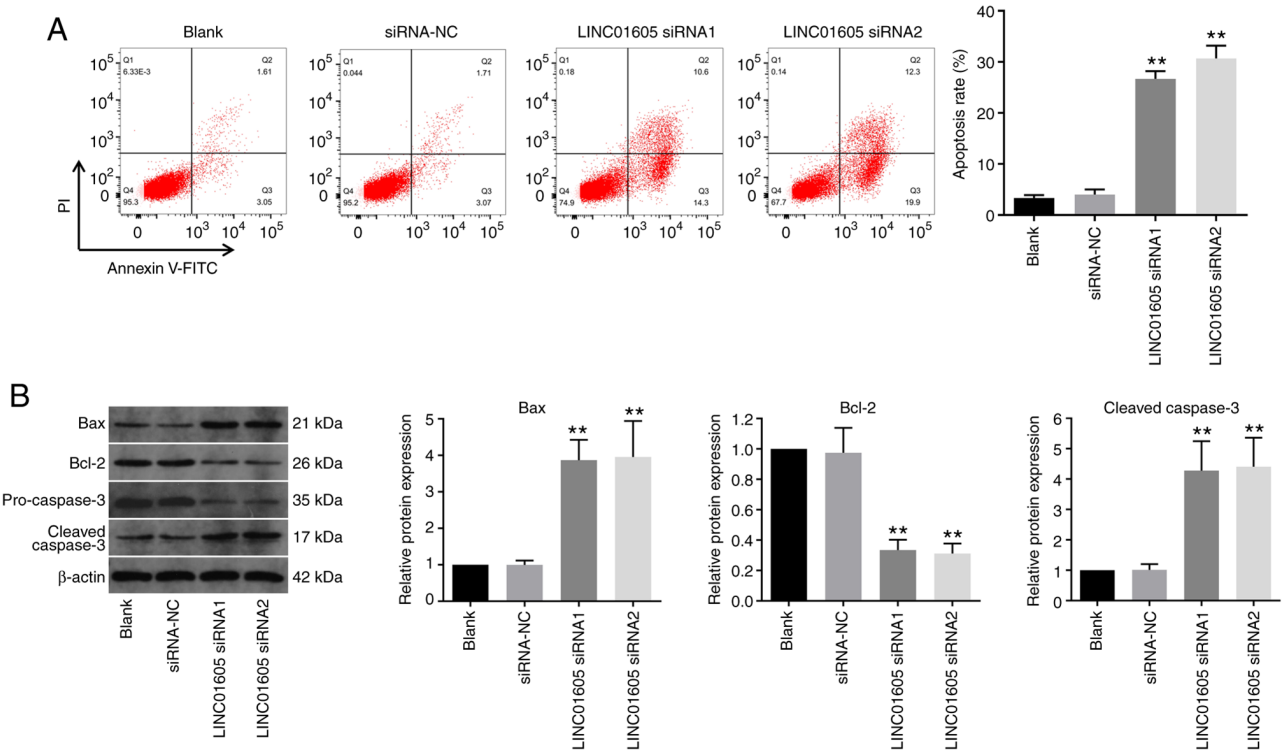

Figure 2. Knockdown of LINC01605 induces HTF apoptosis. (A) HTFs were transfected with siRNA-NC, LINC01605 siRNA1 or LINC01605 siRNA2. Flow cytometry was performed to detect HTF apoptosis. (B) Western blot assays were performed to determine the protein expression levels of Bax, Bcl-2, Pro-caspase-3 and cleaved caspase-3 in HTFs. n=3; **P<0.01 vs. siRNA-NC or blank group. HTFs, human Tenon's capsule fibroblasts; NC, negative control; siRNA, small interfering RNA.

inhibited the migratory ability of HTFs compared with the siRNA-NC or blank group (Fig. 3A). In addition, p-Smad2, α-SMA and MMP9 are important proteins in the process of fibrosis (29-31). Western blot analysis demonstrated that transfection with LINC01605 siRNAs significantly downregulated the ratio of p-Smad2/total Smad2, and the expression levels of α-SMA and MMP9 in HTFs, compared with the siRNA-NC or blank group (Fig. 3B-E). Taken together, these results suggested that LINC01605 knockdown inhibited the migratory ability and the fibrosis process of HTFs.

LINC01605 knockdown inhibits autophagy in HTFs. To determine the association between LINC01605 and autophagy, immunofluorescence staining of LC3 was performed. The results demonstrated that transfection with LINC01605 siRNA significantly decreased LC3 expression in HTFs compared with the siRNA-NC or blank group (Fig. 4A). In addition, the expression levels of autophagy-related proteins were examined. Transfection with LINC01605 siRNAs notably decreased ATG7 and beclin 1 expression, and increased p62 expression in HTFs, compared with the siRNA-NC or blank group (Fig. 4B-E). Since AMPK/mTOR has been reported to serve a crucial role in autophagy, the function of LINC01605 in this signaling pathway was investigated (32,33). Western blotting results demonstrated that transfection with LINC01605 siRNA markedly decreased p-AMPK expression in HTFs compared with the siRNA-NC or Blank group (Fig. 4B and F), indicating that LINC01605 knockdown markedly inhibited autophagy in HTFs. Moreover, it has been reported that 3-methyladenine (3-MA), which is an autophagy inhibitor, could inhibit the formation of autophagosomes (34,35). Given that HTFs were sensitive to LINC01605 siRNA2 (Fig. 1C), it was selected for use in subsequent experiments. LINC01605 siRNA2 significantly inhibited the viability of HTFs compared with the siRNA-NC or blank group, and 3-MA exacerbated this phenomenon (Fig. 4G). These results indicated that LINC01605 knockdown inhibited autophagy in HTFs.

LINC01605 knockdown-induced apoptosis in HTFs is reversed by TGF-β. It has been reported that TGF-β is closely associated with autophagy and fibrosis (36). To further investigate the mechanism by which LINC01605 regulates the formation of HS, rescue experiments were performed. As presented in Fig. 5A and B, LINC01605 knockdown notably inhibited the viability of HTFs by inducing apoptosis, compared with the siRNA-NC or blank group, the effects of which were reversed following treatment with TGF-β. In addition, LINC01605 knockdown notably inhibited the migration of HTFs, compared with siRNA-NC or Blank group, and the effects of which were reversed following treatment with TGF-β (Fig. 5C). Taken together, these results suggested that LINC01605 siRNA2-induced apoptosis of HTFs was reversed by TGF-β.

Discussion

It has been reported that LINC01605 serves an important role in the formation of HS (15). The results of the present study confirmed that LINC01605 expression was upregulated in HS tissues compared with that in healthy tissues. This observation

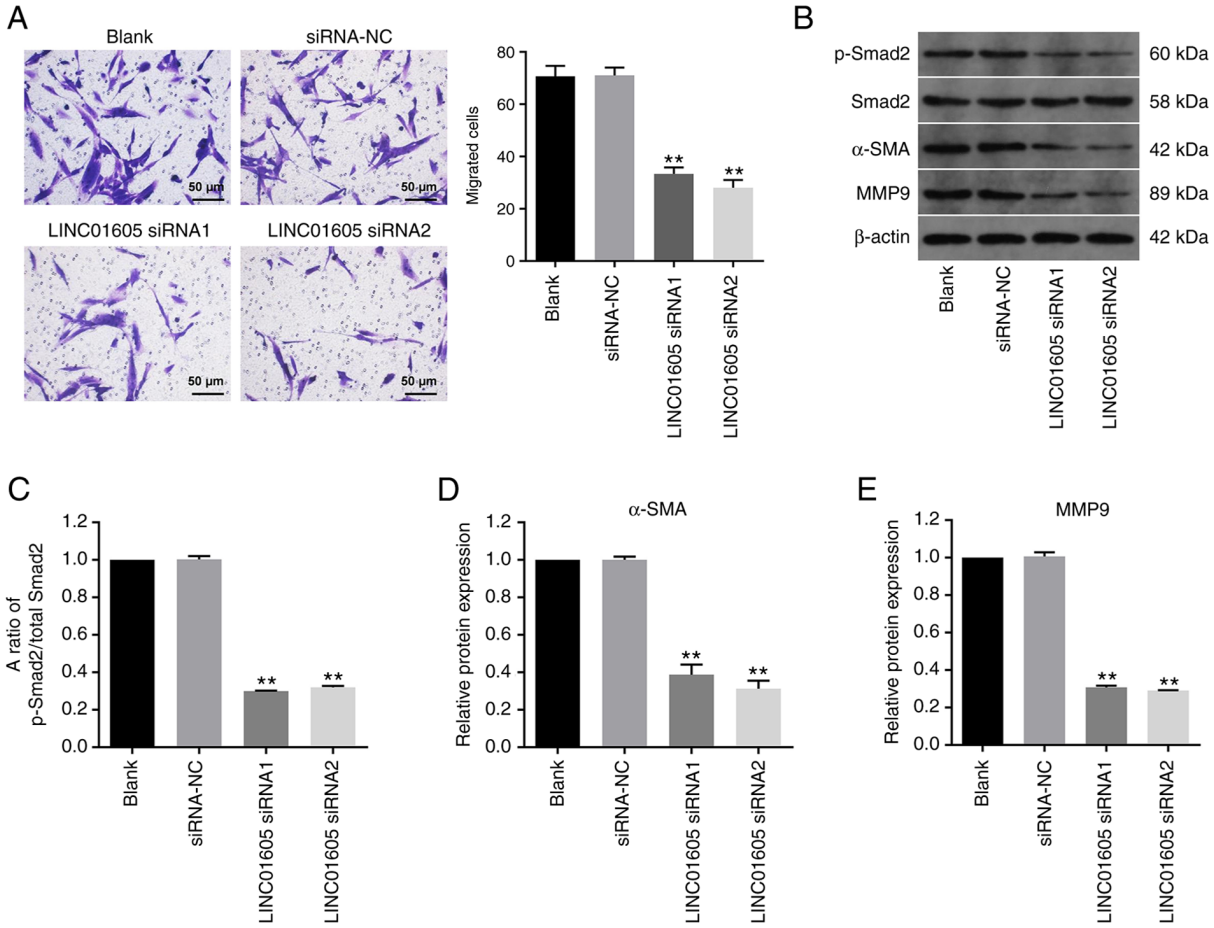

Figure 3. Knockdown of LINC01605 inhibits HTF migration and the marker of fibrotic phenotype (p-Smad2, α-SMA and MMP9). (A) Transwell assay was performed to detect the migratory ability of HTFs. Scale bar, 50 μm. (B) Western blot assays were performed to detect the (C) ratio of p-Smad2/total Smad2, and the expression of (D) α-SMA and (E) MMP9 in HTFs. n=3; **P<0.01 vs. siRNA-NC or blank group. α-SMA, α-smooth muscle actin HTFs, human Tenon's capsule fibroblasts; NC, negative control; p, phosphorylated; siRNA, small interfering RNA.

was similar to that published in a previous study (37). In the present study, LINC01605 was knocked down, which inhibited HTF migration and fibrotic phenotype, induced apoptosis and inhibited autophagy. Overexpression of LINC01605 has been indicated to promote the migration of bladder cancer cells (38); moreover, Zhu *et al* (15) reported that blocking LINC01605 inhibited the M2 macrophage-induced migration, invasion and proliferation of human dermal fibroblasts. In the present study, it was found that knockdown of LINC01605 inhibited HTF migration and fibrotic phenotype. The present study results were consistent with previous reports (15).

A previous study reported that the formation of HS was attributed to the inhibition of apoptosis in p53-deficient mice (39). During the formation and development of HS, cell proliferation and migration are promoted, and apoptosis is inhibited (40). The present study assessed Bax, Bcl-2 and cleaved caspase-3 as apoptosis-related proteins (41-43). The results demonstrated that LINC01605 knockdown significantly induced the apoptosis of HTFs, which was consistent with previous findings (39,40).

LC3 is widely used for the detection of autophagy levels (44-46). When autophagy increases, the number of LC3 puncta in cells significantly increase (47). In the present study, LINC01605 knockdown notably decreased LC3 expression in HTFs, suggesting that autophagy was inhibited in HTF. In addition, it is well known that the association between apoptosis and autophagy is highly complex (48-50). For example, Chakrabarti and Ray (51) indicated that the natural flavonoid luteolin induced glioblastoma cell apoptosis by inhibiting autophagy. Moreover, Cao *et al* (52) reported that autophagy inhibitors could promote apoptosis and thus effectively inhibit the formation of HS. In addition, Deng *et al* (53) demonstrated that oxymatrine, an alkaloid isolated from plants, was able to promote HS repair by inhibiting autophagy and inducing apoptosis. Based on the results of the present study, it was suggested that LINC01605 knockdown may induce the apoptosis of HTFs by inhibiting autophagy, which is consistent with previous research (51-53). In addition, the present study results indicated that LINC01605 knockdown downregulated the expression levels of p-Smad2, α-SMA and MMP9 in HTFs. Proteins (α-SMA and MMP9) that affect the Smad pathway and induce epithelial-mesenchymal transition are involved in fibrosis (54,55). Notably, in the present study, the results (p-Smad2, α-SMA and MMP9 expression, characteristic of fibrosis/fibrotic phenotype) indicated that LINC01605 knockdown inhibited the fibrotic phenotype of HTFs.

TGF-β is closely associated with autophagy and fibrosis (36). For example, autophagy can downregulate

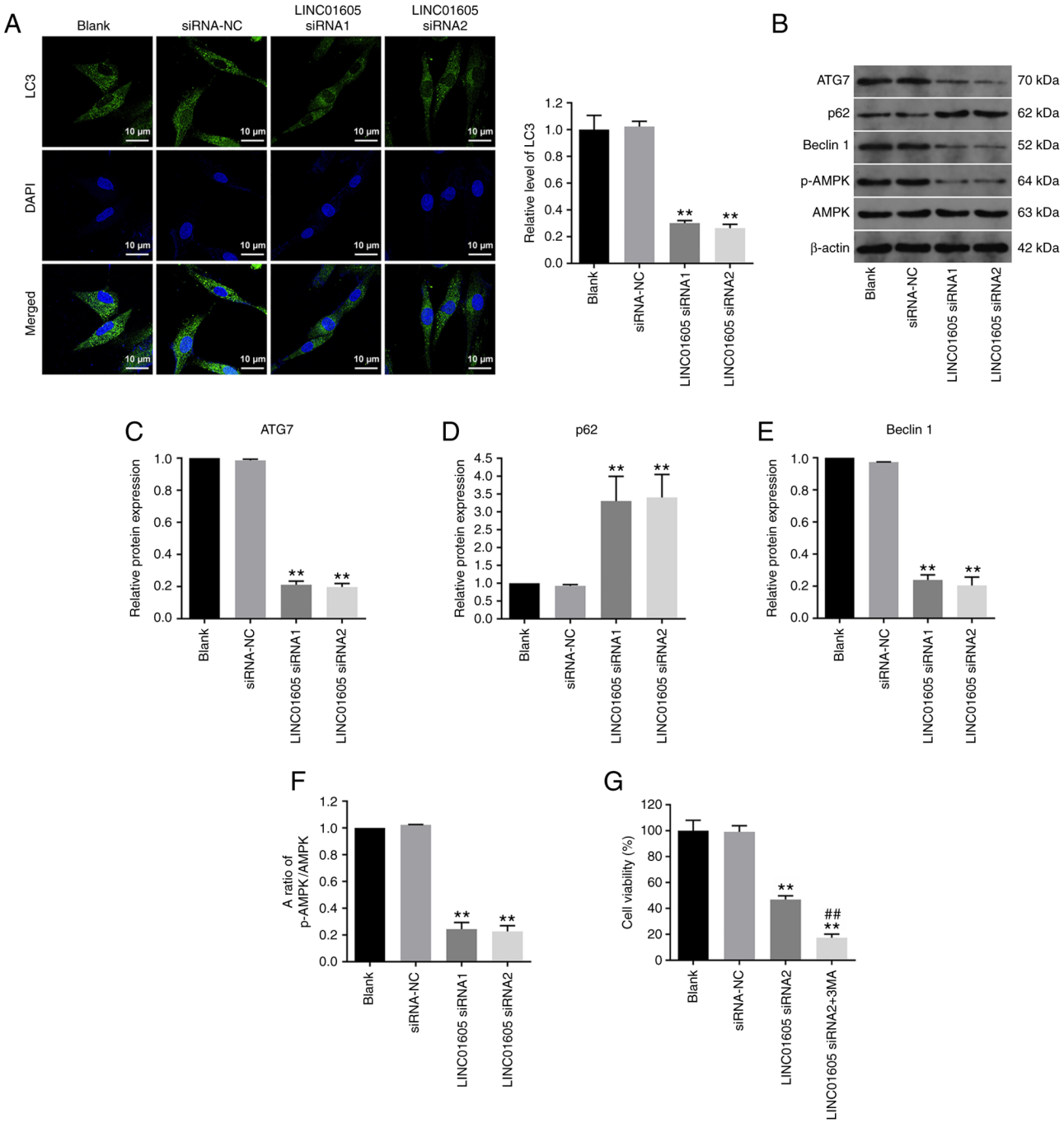

Figure 4. Knockdown of LINC01605 inhibits HTF autophagy. (A) Immunofluorescence staining was performed to detect the expression of LC3 in HTFs. Scale bar, 10 μm. (B) Western blot assays were performed to detect and semi-quantify the expression levels of (C) ATG7, (D) p62, (E) beclin 1, (F) p-AMPK and AMPK in HTFs. (G) Cell Counting Kit-8 assay was used to detect the viability of HTFs. n=3; **P<0.01 vs. siRNA-NC or Blank group; $^{\#\#}$P<0.01 vs. LINC01605 siRNA2 group. AMPK, AMP-activated protein kinase; ATG7, autophagy-related 7; HTFs, human Tenon's capsule fibroblasts; NC, negative control; p, phosphorylated; siRNA, small interfering RNA.

TGF-β expression and inhibit renal fibrosis (56). In addition, Wu *et al* (57) indicated that quercetin, a natural flavonoid, prevented liver fibrosis by inhibiting autophagy. Moreover, Liu *et al* (58) reported that isorhamnetin, which is a flavonol aglycone isolated from the plant *Hippophae rhamnoides L.*, could also inhibit liver fibrosis by reducing autophagy. All these data suggested that TGF-β and autophagy serve an important role in the process of fibrosis. Therefore, these results collectively suggested that TGF-β, autophagy and fibrosis are closely related. Thus, TGF-β was used to perform rescue experiments in the present study.

The present study has certain limitations. For example, the mechanism through which LINC01605 regulates the Smad pathway remains unclear. In addition, the association between LINC01605 and cell autophagy has not been extensively investigated. RNA *in situ* hybridization of LINC01605 in the patients' tissue sections could not be provided owing to limited experimental conditions. Moreover, the expression levels of LINC01605 among patients with POAG at different disease

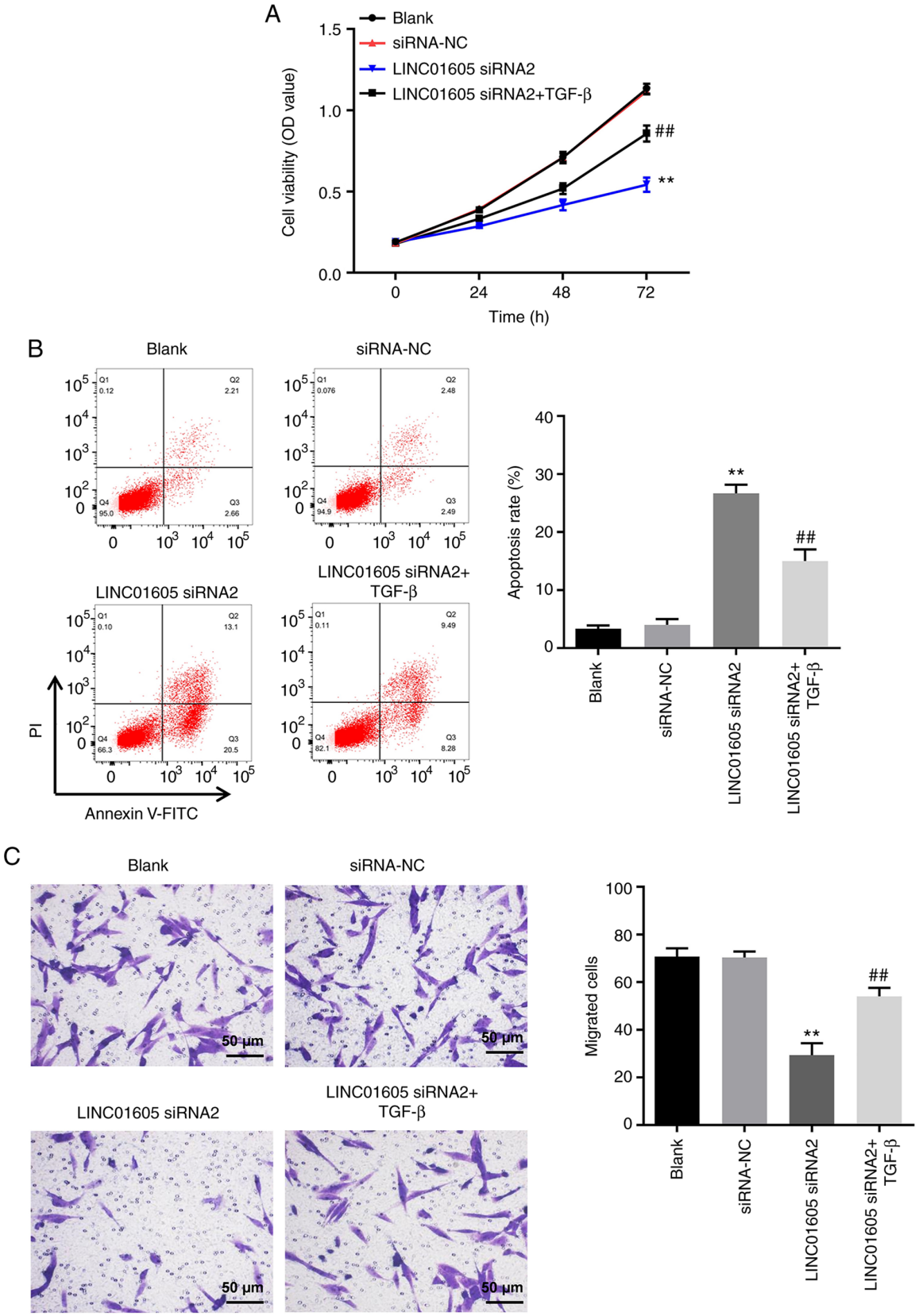

Figure 5. LINC01605 siRNA2-induced apoptosis of HTFs is reversed by TGF-β. HTFs were transfected with siRNA-NC, LINC01605 siRNA2 or LINC01605 siRNA2 + TGF-β. (A) Cell Counting Kit-8 assay was used to detect the viability of transfected HTFs. (B) Flow cytometry was used to determine apoptotic rates. (C) Transwell assay was performed to examine the migratory ability of the transfected HTFs. Scale bar, 50 μm. n=3; **P<0.01 vs. siRNA-NC or blank group; $^{\#\#}$P<0.01 vs. LINC01605 siRNA2 group. HTFs, human Tenon's capsule fibroblasts; NC, negative control; OD, optical density; siRNA, small interfering RNA.

stages could not be compared owing to the lack of adequate samples at different disease stages.

In conclusion, results from the present study demonstrated that LINC01605 knockdown inhibited the viability of

HTFs by inducing apoptosis and suggested that LINC01605 knockdown may provide novel directions for the treatment of HS.

Acknowledgements

Not applicable.

Funding

No funding was received.

Availability of data and materials

The datasets used and/or analyzed during the current study are available from the corresponding author on reasonable request.

Authors' contributions

QS made major contributions to the conception and design of the study, as well as drafting and revising the manuscript. YY and HL were responsible for data acquisition, including conducting the experiments, data analysis, data interpretation and manuscript revision. QS, YY and HL confirm the authenticity of all the raw data. All authors agreed to be accountable for all aspects of the work. All authors have read and approved the final manuscript.

Ethics approval and consent to participate

The present study was approved by the Ethics Committee of Fuyang People's Hospital (Hangzhou, China), and written informed consent was provided by all patients prior to the study start.

Patient consent for publication

Not applicable.

Competing interests

The authors declare that they have no competing interests.

References

1. Bluwol E: Glaucoma treatment. Rev Prat 66: 508-513, 2016 (In French).
2. Weinreb RN, Aung T and Medeiros FA: The pathophysiology and treatment of glaucoma: A review. JAMA 311: 1901-1911, 2014.
3. Sihota R, Angmo D, Ramaswamy D and Dada T: Simplifying 'target' intraocular pressure for different stages of primary open-angle glaucoma and primary angle-closure glaucoma. Indian J Ophthalmol 66: 495-505, 2018.
4. Swogger J, Conner IP, Rosano M, Kemmerer M, Happ-Smith C, Wells A, Schuman JS and Yates CC: Injected versus sponge-applied mitomycin C (MMC) during modified trabeculectomy in New Zealand white rabbit model. Transl Vis Sci Technol 9: 23, 2020.
5. Vajaranant TS, Wu S, Torres M and Varma R: The changing face of primary open-angle glaucoma in the United States: Demographic and geographic changes from 2011 to 2050. Am J Ophthalmol 154: 303-314.e3, 2012.
6. Ma X and Liu L: Knockdown of FAM225B inhibits the progression of the hypertrophic scar following glaucoma surgery by inhibiting autophagy. Mol Med Rep 23: 204, 2021.
7. Wu X, Wang Z, Wu G, Xu X, Zhang J, Li Y, Zhang H and Guo S: Tetramethylpyrazine induces apoptosis and inhibits proliferation of hypertrophic scar-derived fibroblasts via inhibiting the phosphorylation of AKT. Front Pharmacol 11: 602, 2020.
8. Lee HJ and Jang YJ: Recent understandings of biology, prophylaxis and treatment strategies for hypertrophic scars and keloids. Int J Mol Sci 19: 711, 2018.
9. Wang P, Luo ML, Song E, Zhou Z, Ma T, Wang J, Jia N, Wang G, Nie S, Liu Y and Hou F: Long noncoding RNA lnc-TSI inhibits renal fibrogenesis by negatively regulating the TGF-β/Smad3 pathway. Sci Transl Med 10: eaat2039, 2018.
10. Jiang R, Tang J, Chen Y, Deng L, Ji J, Xie Y, Wang K, Jia W, Chu WM and Sun B: The long noncoding RNA lnc-EGFR stimulates T-regulatory cells differentiation thus promoting hepatocellular carcinoma immune evasion. Nat Commun 8: 15129, 2017.
11. Zheng M, Zheng Y, Gao M, Ma H, Zhang X, Li Y, Wang F and Huang H: Expression and clinical value of lncRNA MALAT1 and lncRNA ANRIL in glaucoma patients. Exp Ther Med 19: 1329-1335, 2020.
12. Cissé Y, Bai L and Meng T: LncRNAs in genetic basis of glaucoma. BMJ Open Ophthalmol 3: e000131, 2018.
13. Nong Q, Li S, Wu Y and Liu D: LncRNA COL1A2-AS1 inhibits the scar fibroblasts proliferation via regulating miR-21/Smad7 pathway. Biochem Biophys Res Commun 495: 319-324, 2018.
14. Li J, Chen L, Cao C, Yan H, Zhou B, Gao Y, Li Q and Li J: The long non-coding RNA LncRNA8975-1 is upregulated in hypertrophic scar fibroblasts and controls collagen expression. Cell Physiol Biochem 40: 326-334, 2016.
15. Zhu Z, Chen B, Peng L, Gao S, Guo J and Zhu X: Blockade of LINC01605-enriched exosome generation in M2 macrophages impairs M2 macrophage-induced proliferation, migration, and invasion of human dermal fibroblasts. Int J Immunopathol Pharmacol 35: 20587384211016724, 2021.
16. Wang XC, Wang T, Zhang Y, Wang LL, Zhao RY and Tan W: Tacrolimus inhibits proliferation and induces apoptosis by decreasing survivin in scar fibroblasts after glaucoma surgery. Eur Rev Med Pharmacol Sci 22: 2934-2940, 2018.
17. Jammal AA, Berchuck SI, Thompson AC, Costa VP and Medeiros FA: The effect of age on increasing susceptibility to retinal nerve fiber layer loss in glaucoma. Invest Ophthalmol Vis Sci 61: 8, 2020.
18. Deflorin C, Hohenauer E, Stoop R, van Daele U, Clijsen R and Taeymans J: Physical management of scar tissue: A systematic review and meta-analysis. J Altern Complement Med 26: 854-865, 2020.
19. Seong GJ, Hong S, Jung SA, Lee JJ, Lim E, Kim SJ and Lee JH: TGF-beta-induced interleukin-6 participates in transdifferentiation of human Tenon's fibroblasts to myofibroblasts. Mol Vis 15: 2123-2128, 2009.
20. Trelford CB, Denstedt JT, Armstrong JJ and Hutnik CML: The pro-fibrotic behavior of human Tenon's capsule fibroblasts in medically treated glaucoma patients. Clin Ophthalmol 14: 1391-1402, 2020.
21. Ran W, Zhu D and Feng Q: TGF-β2 stimulates Tenon's capsule fibroblast proliferation in patients with glaucoma via suppression of miR-29b expression regulated by Nrf2. Int J Clin Exp Pathol 8: 4799-4806, 2015.
22. Song L, Liu H, Ma L, Zhang X, Jiang Z and Jiang C: Inhibition of autophagy by 3-MA enhances endoplasmic reticulum stress-induced apoptosis in human nasopharyngeal carcinoma cells. Oncol Lett 6: 1031-1038, 2013.
23. Wang J, Xiao L, Luo CH, Zhou H, Zeng L, Zhong J, Tang Y, Zhao XH, Zhao M and Zhang Y: CD44v6 promotes β-catenin and TGF-β expression, inducing aggression in ovarian cancer cells. Mol Med Rep 11: 3505-3510, 2015.
24. Wang T, Gao X, Chen S, Li D, Chen S, Xie M, Xu Z and Yang G: Genome-wide identification and expression analysis of ethylene responsive factor family transcription factors in Juglans regia. PeerJ 9: e12429, 2021.
25. Lassance L, Marino GK, Medeiros CS, Thangavadivel S and Wilson SE: Fibrocyte migration, differentiation and apoptosis during the corneal wound healing response to injury. Exp Eye Res 170: 177-187, 2018.
26. Battaglia RA, Delic S, Herrmann H and Snider NT: Vimentin on the move: New developments in cell migration. F1000Res 7: F1000 Faculty Rev-1796, 2018.

27. Patteson AE, Carroll RJ, Iwamoto DV and Janmey PA: The vimentin cytoskeleton: When polymer physics meets cell biology. Phys Biol 18: 011001, 2020.
28. Polari L, Alam CM, Nyström JH, Heikkilä T, Tayyab M, Baghestani S and Toivola DM: Keratin intermediate filaments in the colon: Guardians of epithelial homeostasis. Int J Biochem Cell Biol 129: 105878, 2020.
29. Wu Y, Lu S, Huang X, Liu Y, Huang K, Liu Z, Xu W, Zhu W, Hou J, Liu H and Zhang X: Targeting cIAPs attenuates CCl(4)-induced liver fibrosis by increasing MMP9 expression derived from neutrophils. Life Sci 289: 120235, 2022.
30. Li CY, Zhang JR, Li XX, Zhao L, Xi H, Hu WN and Li SN: Lefty1 ameliorates post-infarction fibrosis by suppressing p-Smad2 and p-ERK1/2 signaling pathways. J Cardiovasc Transl Res 14: 636-646, 2021.
31. Chang J, Lan T, Li C, Ji X, Zheng L, Gou H, Ou Y, Wu T, Qi C, Zhang Q, *et al*: Activation of Slit2-Robo1 signaling promotes liver fibrosis. J Hepatol 63: 1413-1420, 2015.
32. Li MY, Zhu XL, Zhao BX, Shi L, Wang W, Hu W, Qin SL, Chen BH, Zhou PH, Qiu B, *et al*: Adrenomedullin alleviates the pyroptosis of Leydig cells by promoting autophagy via the ROS-AMPK-mTOR axis. Cell Death Dis 10: 489, 2019.
33. Han D, Jiang L, Gu X, Huang S, Pang J, Wu Y, Yin J and Wang J: SIRT3 deficiency is resistant to autophagy-dependent ferroptosis by inhibiting the AMPK/mTOR pathway and promoting GPX4 levels. J Cell Physiol 235: 8839-8851, 2020.
34. Cao H, Jia Q, Yan L, Chen C, Xing S and Shen D: Quercetin suppresses the progression of atherosclerosis by regulating MST1-mediated autophagy in ox-LDL-Induced RAW264.7 macrophage foam cells. Int J Mol Sci 20: 6093, 2019.
35. He Z, Guo L, Shu Y, Fang Q, Zhou H, Liu Y, Liu D, Lu L, Zhang X, Ding X, *et al*: Autophagy protects auditory hair cells against neomycin-induced damage. Autophagy 13: 1884-1904, 2017.
36. Xia Y, Li J, Chen K, Feng J and Guo C: Bergenin attenuates hepatic fibrosis by regulating autophagy mediated by the PPAR-γ/TGF-β pathway. PPAR Res 2020: 6694214, 2020.
37. Wang X, Song W, Zhang F and Huang R: Dihydroartemisinin Inhibits TGF-β-induced fibrosis in human tenon fibroblasts via inducing autophagy. Drug Des Devel Ther 15: 973-981, 2021.
38. Correction: High LINC01605 expression predicts poor prognosis and promotes tumor progression via upregulation of MMP9 in bladder cancer. Biosci Rep 40: BSR-20180562_COR, 2020.
39. Aarabi S, Bhatt KA, Shi Y, Paterno J, Chang EI, Loh SA, Holmes JW, Longaker MT, Yee H and Gurtner GC: Mechanical load initiates hypertrophic scar formation through decreased cellular apoptosis. FASEB J 21: 3250-3261, 2007.
40. Jiang D, Guo B, Lin F, Lin S and Tao K: MiR-205 inhibits the development of hypertrophic scars by targeting THBS1. Aging (Albany NY) 12: 22046-22058, 2020.
41. Zhang Y, Yang X, Ge X and Zhang F: Puerarin attenuates neurological deficits via Bcl-2/Bax/cleaved caspase-3 and Sirt3/SOD2 apoptotic pathways in subarachnoid hemorrhage mice. Biomed Pharmacother 109: 726-733, 2019.
42. Dolka I, Król M and Sapierzyński R: Evaluation of apoptosis-associated protein (Bcl-2, Bax, cleaved caspase-3 and p53) expression in canine mammary tumors: An immunohistochemical and prognostic study. Res Vet Sci 105: 124-133, 2016.
43. Zhao T, Fu Y, Sun H and Liu X: Ligustrazine suppresses neuron apoptosis via the Bax/Bcl-2 and caspase-3 pathway in PC12 cells and in rats with vascular dementia. IUBMB Life 70: 60-70, 2018.
44. Tanida I, Ueno T and Kominami E: LC3 and autophagy. Methods Mol Biol 445: 77-88, 2008.
45. Schaaf MB, Keulers TG, Vooijs MA and Rouschop KM: LC3/GABARAP family proteins: Autophagy-(un)related functions. FASEB J 30: 3961-3978, 2016.
46. Tanida I, Ueno T and Kominami E: LC3 conjugation system in mammalian autophagy. Int J Biochem Cell Biol 36: 2503-2518, 2004.
47. Runwal G, Stamatakou E, Siddiqi FH, Puri C, Zhu Y and Rubinsztein DC: LC3-positive structures are prominent in autophagy-deficient cells. Sci Rep 9: 10147, 2019.
48. Maiuri MC, Zalckvar E, Kimchi A and Kroemer G: Self-eating and self-killing: Crosstalk between autophagy and apoptosis. Nat Rev Mol Cell Biol 8: 741-752, 2007.
49. Fernández A, Ordóñez R, Reiter RJ, González-Gallego J and Mauriz JL: Melatonin and endoplasmic reticulum stress: Relation to autophagy and apoptosis. J Pineal Res 59: 292-307, 2015.
50. Lv W, Jiang J, Li Y, Fu L, Meng F and Li J: MiR-302a-3p aggravates myocardial ischemia-reperfusion injury by suppressing mitophagy via targeting FOXO3. Exp Mol Pathol 117: 104522, 2020.
51. Chakrabarti M and Ray SK: Anti-tumor activities of luteolin and silibinin in glioblastoma cells: Overexpression of miR-7-1-3p augmented luteolin and silibinin to inhibit autophagy and induce apoptosis in glioblastoma in vivo. Apoptosis 21: 312-328, 2016.
52. Cao C, Wang W, Lu L, Wang L, Chen X, Guo R, Li S and Jiang J: Inactivation of Beclin-1-dependent autophagy promotes ursolic acid-induced apoptosis in hypertrophic scar fibroblasts. Exp Dermatol 27: 58-63, 2018.
53. Deng X, Zhao F, Zhao D, Zhang Q, Zhu Y, Chen Q, Qiang L, Xie N, Ma J, Pan X, *et al*: Oxymatrine promotes hypertrophic scar repair through reduced human scar fibroblast viability, collagen and induced apoptosis via autophagy inhibition. Int Wound J: Nov 8, 2021 (Epub ahead of print).
54. Jia L, Sun P, Gao H, Shen J, Gao Y, Meng C, Fu S, Yao H and Zhang G: Mangiferin attenuates bleomycin-induced pulmonary fibrosis in mice through inhibiting TLR4/p65 and TGF-β1/Smad2/3 pathway. J Pharm Pharmacol 71: 1017-1028, 2019.
55. Zhang Q, Chang X, Wang H, Liu Y, Wang X, Wu M, Zhan H, Li S and Sun Y: TGF-β1 mediated Smad signaling pathway and EMT in hepatic fibrosis induced by Nano NiO in vivo and in vitro. Environ Toxicol 35: 419-429, 2020.
56. Nam SA, Kim WY, Kim JW, Park SH, Kim HL, Lee MS, Komatsu M, Ha H, Lim JH, Park CW, *et al*: Autophagy attenuates tubulointerstital fibrosis through regulating transforming growth factor-β and NLRP3 inflammasome signaling pathway. Cell Death Dis 10: 78, 2019.
57. Wu L, Zhang Q, Mo W, Feng J, Li S, Li J, Liu T, Xu S, Wang W, Lu X, *et al*: Quercetin prevents hepatic fibrosis by inhibiting hepatic stellate cell activation and reducing autophagy via the TGF-β1/Smads and PI3K/Akt pathways. Sci Rep 7: 9289, 2017.
58. Liu N, Feng J, Lu X, Yao Z, Liu Q, Lv Y, Han Y, Deng J and Zhou Y: Isorhamnetin inhibits liver fibrosis by reducing autophagy and inhibiting extracellular matrix formation via the TGF-β1/Smad3 and TGF-β1/p38 MAPK pathways. Mediators Inflamm 2019: 6175091, 2019.